

¹ PeriDEM – High-fidelity modeling of granular media consisting of deformable complex-shaped particles

³ **Prashant K. Jha**  ¹

⁴ 1 Department of Mechanical Engineering, South Dakota School of Mines and Technology, Rapid City,
⁵ SD 57701, USA

DOI: [10.xxxxxx/draft](https://doi.org/10.xxxxxx/draft)

Software

- [Review](#) 
- [Repository](#) 
- [Archive](#) 

Editor: [Open Journals](#) 

Reviewers:

- [@openjournals](#)

Submitted: 01 January 1970

Published: unpublished

License

Authors of papers retain copyright and release the work under a Creative Commons Attribution 4.0 International License ([CC BY 4.0](#))¹⁷¹⁸

⁶ Summary

⁷ Accurate simulation of granular materials under extreme mechanical conditions, such as crushing, fracture, and large deformation, remains a significant challenge in geotechnical, manufacturing, and mining applications. Classical discrete element method (DEM) models typically treat particles as rigid or nearly rigid bodies, limiting their ability to capture internal deformation and fracture. The PeriDEM library, first introduced in ([Prashant K. Jha et al., 2021](#)), addresses this limitation by modeling particles as deformable solids using peridynamics, a nonlocal continuum theory that naturally accommodates fracture and significant deformation. Inter-particle contact is handled using DEM-inspired local laws, enabling realistic interaction between complex-shaped particles.¹⁰¹¹¹²¹³¹⁴¹⁵

¹⁶ Implemented in C++, PeriDEM is designed for extensibility and ease of deployment. It relies on a minimal set of external libraries, supports multithreaded execution, and includes demonstration examples involving compaction, fracture, and rotational dynamics. The framework facilitates granular-scale simulations, supports the development of constitutive models, and serves as a foundation for multi-fidelity coupling in real-world applications.¹⁷¹⁸¹⁹²⁰²¹²²²³²⁴²⁵²⁶²⁷²⁸²⁹³⁰³¹³²³³³⁴³⁵³⁶³⁷³⁸³⁹⁴⁰

²¹ Statement of Need

²² Granular materials play a central role in many engineered systems, but modeling their behavior under high loading, deformation, and fragmentation remains an open problem. Popular open-source DEM codes such as YADE ([Smilauer et al., 2021](#)), BlazeDEM ([Govender et al., 2016](#)), Chrono DEM-Engine ([Zhang et al., 2024](#)), and LAMMPS ([Thompson et al., 2022](#)) are widely used but typically treat particles as rigid, limiting their accuracy in scenarios involving internal deformation and breakage. A recent review by Dosta et al. ([Dosta et al., 2024](#)) compares several DEM libraries. Meanwhile, peridynamics-based codes such as Peridigm ([Littlewood et al., 2024](#)) and NLMech ([Prashant K. Jha & Diehl, 2021](#)) are designed to simulate deformation and fracture within a single structure, with limited support for multi-structure simulations.²³²⁴²⁵²⁶²⁷²⁸²⁹³⁰³¹³²³³³⁴³⁵³⁶³⁷³⁸³⁹⁴⁰

³¹ PeriDEM fills this gap by integrating state-based peridynamics for intra-particle deformation with DEM-style contact laws for particle interactions. This hybrid approach enables direct simulation of particle fragmentation, stress redistribution, and dynamic failure propagation—capabilities essential for modeling granular compaction, attrition, and crushing.³²³³³⁴³⁵³⁶³⁷³⁸³⁹⁴⁰

³⁵ Recent multiscale approaches, including DEM-continuum and DEM-level-set coupling methods ([Harmon et al., 2021](#)), aim to bridge scales but often rely on homogenization assumptions. Sand crushing in geotechnical systems, for example, has been modeled using micro-CT-informed FEM or phenomenological laws ([Chen et al., 2023](#)). PeriDEM offers a particle-resolved alternative that allows bottom-up investigation of granular failure and shape evolution, especially in systems where fragment dynamics are critical.³⁶³⁷³⁸³⁹⁴⁰

41 Background

42 The PeriDEM model was introduced in ([Prashant K. Jha et al., 2021](#)), demonstrating its
 43 ability to model inter-particle contact and intra-particle fracture for complex-shaped particles.
 44 It is briefly described next.

45 Brief Introduction to PeriDEM Model

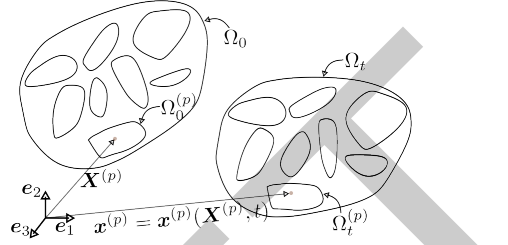


Figure 1: Motion of particle system.

46 Consider a fixed frame of reference and $\{e_i\}_{i=1}^d$ are orthonormal bases. Consider a collection
 47 of N_P particles $\Omega_0^{(p)}$, $1 \leq p \leq N_P$, where $\Omega_0^{(p)} \subset \mathbb{R}^d$ with $d = 2, 3$ represents the initial
 48 configuration of particle p . Suppose $\Omega_0 \supset \cup_{p=1}^{N_P} \Omega_0^{(p)}$ is the domain containing all particles; see
 49 [Figure 1](#). The particles in Ω_0 are dynamically evolving due to external boundary conditions and
 50 internal interactions; let $\Omega_t^{(p)}$ denote the configuration of particle p at time $t \in (0, t_F]$, and
 51 $\Omega_t \supset \cup_{p=1}^{N_P} \Omega_t^{(p)}$ domain containing all particles at that time. The motion $x^{(p)} = x^{(p)}(\mathbf{X}^{(p)}, t)$
 52 takes point $\mathbf{X}^{(p)} \in \Omega_0^{(p)}$ to $x^{(p)} \in \Omega_t^{(p)}$, and collectively, the motion is given by $\mathbf{x} = \mathbf{x}(\mathbf{X}, t) \in$
 53 Ω_t for $\mathbf{X} \in \Omega_0$. We assume the media is dry and not influenced by factors other than
 54 mechanical loading (e.g., moisture and temperature are not considered). The configuration of
 55 particles in Ω_t at time t depends on various factors, such as material and geometrical properties,
 56 contact mechanism, and external loading. Essentially, there are two types of interactions
 57 present in the media:

- 58 ▪ *Intra-particle interaction* that models the deformation and internal forces in the particle
 59 and
- 60 ▪ *Inter-particle interaction* that accounts for the contact between particles and the boundary
 61 of the domain in which the particles are contained.

62 In DEM, the first interaction is ignored, assuming that particle deformation is insignificant
 63 compared to inter-particle interactions. On the other hand, PeriDEM accounts for both
 64 interactions.

65 The balance of linear momentum for particle p , $1 \leq p \leq N_P$, takes the form:

$$\rho^{(p)} \ddot{\mathbf{u}}^{(p)}(\mathbf{X}, t) = \mathbf{f}_{int}^{(p)}(\mathbf{X}, t) + \mathbf{f}_{ext}^{(p)}(\mathbf{X}, t), \quad \forall (\mathbf{X}, t) \in \Omega_0^{(p)} \times (0, t_F), \quad (1)$$

66 where $\rho^{(p)}$, $\mathbf{f}_{int}^{(p)}$, and $\mathbf{f}_{ext}^{(p)}$ are density, and internal and external force densities. The
 67 above equation is complemented with initial conditions, $\mathbf{u}^{(p)}(\mathbf{X}, 0) = \mathbf{u}_0^{(p)}(\mathbf{X})$, $\dot{\mathbf{u}}^{(p)}(\mathbf{X}, 0) =$
 68 $\dot{\mathbf{u}}_0^{(p)}(\mathbf{X})$, $\mathbf{X} \in \Omega_0^{(p)}$.

69 Internal force – State-based peridynamics

70 The internal force term $\mathbf{f}_{int}^{(p)}(\mathbf{X}, t)$ in the momentum balance governs intra-particle deformation
 71 and fracture. In PeriDEM, this term is modeled using a simplified state-based peridynamics
 72 formulation that accounts for nonlocal interactions over a finite horizon. The underlying model

⁷³ and its numerical implementation are discussed in detail in [(Prashant K. Jha et al., 2021),
⁷⁴ Sections 2.1 and 2.3].

⁷⁵ DEM-inspired contact forces

⁷⁶ The external force term $f_{ext}^{(p)}(X, t)$ includes body forces, wall-particle interactions, and contact
⁷⁷ forces from other particles. Contact is modeled using a spring-dashpot-slider formulation
⁷⁸ applied locally when particles come within a critical distance; see Figure 2. This approach
⁷⁹ introduces nonlinear normal forces, damping, and friction without relying on particle convexity
⁸⁰ or geometric simplifications. The full formulation of contact detection, force assembly, and
⁸¹ implementation is detailed in [(Prashant K. Jha et al., 2021), Section 2.2].

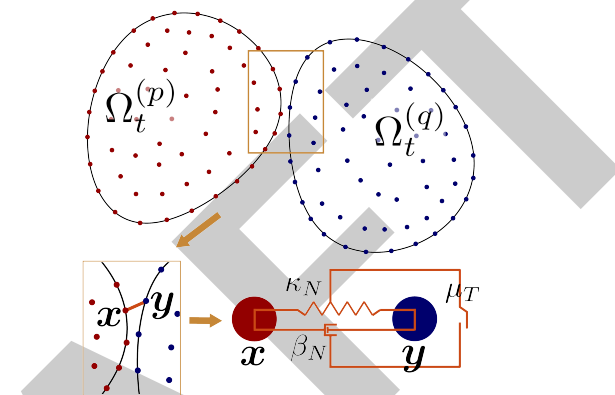


Figure 2: High-resolution contact approach in PeriDEM model for granular materials? between arbitrarily-shaped particles. The spring-dashpot-slider system shows the normal contact (spring), normal damping (dashpot), and tangential friction (slider) forces between points x and y .

⁸² Implementation

⁸³ PeriDEM is implemented in C++ and hosted on GitHub. It depends on a minimal set of
⁸⁴ external libraries, most of which are bundled in the external directory. Key dependencies
⁸⁵ include Taskflow (Huang et al., 2021) for multithreaded parallelism, nanoflann (Blanco &
⁸⁶ Rai, 2014) for efficient neighborhood search, and VTK for output. The numerical strategies
⁸⁷ for neighbor search, peridynamic integration, damage evaluation, and time stepping follow
⁸⁸ those introduced in [(Prashant K. Jha et al., 2021), Section 3]. The core simulation model
⁸⁹ is implemented in `src/model/dem`, with the class `DEMModel` managing particle states, force
⁹⁰ calculations, and time integration. This work builds on earlier research in the analysis and
⁹¹ numerical methods for peridynamics; see (Prashant K. Jha et al., 2025; Prashant K. Jha &
⁹² Lipton, 2018a, 2018b, 2019; Prashant K. Jha & Lipton, 2020).

⁹³ Features

- ⁹⁴ ▪ Combines peridynamics and DEM to model intra-particle deformation and inter-particle contact
- ⁹⁵
- ⁹⁶ ▪ Simulates deformation and breakage of single particles under complex loading conditions
- ⁹⁷
- ⁹⁸ ▪ Supports arbitrarily shaped particles for realistic granular systems
- ⁹⁹
- ¹⁰⁰ ▪ Ongoing development of MPI-based parallelism and adaptive modeling strategies to
¹⁰¹ improve efficiency without sacrificing accuracy
- ¹⁰²

103 Examples

104 Example cases are described in [examples/README.md](#). One key simulation demonstrates
 105 the compression of over 500 circular and hexagonal particles in a rectangular container by
 106 displacing the top wall. The stress on the wall becomes increasingly nonlinear with penetration
 107 depth as damage accumulates and the medium yields (see [Figure 3a](#)).

108 Preliminary performance tests show that compute time increases exponentially with particle
 109 count due to the nonlocal nature of both peridynamic and contact interactions—highlighting
 110 a computational bottleneck. This motivates future integration of MPI-based parallelism and
 111 a multi-fidelity modeling framework. Additional examples include attrition of non-circular
 112 particles in a rotating cylinder ([Figure 3c](#)).

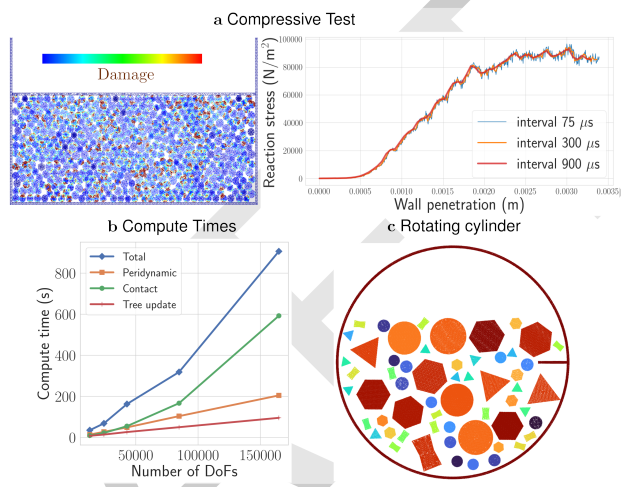


Figure 3: (a) Nonlinear response under compression, (b) exponential growth of compute time due to nonlocality of internal and contact forces, and (c) rotating cylinder with nonspherical particles.

113 Acknowledgements

114 This work was supported by the U.S. National Science Foundation through the Engineering
 115 Research Initiation (ERI) program under Grant No. 2502279. The support has contributed to
 116 the continued development and enhancement of the PeriDEM library.

117 References

- 118 Blanco, J. L., & Rai, P. K. (2014). *Nanoflann: A C++ header-only fork of FLANN, a library*
 119 *for nearest neighbor (NN) with KD-trees*. <https://github.com/jlblancoc/nanoflann>.
- 120 Chen, Q., Li, Z., Dai, Z., Wang, X., Zhang, C., & Zhang, X. (2023). Mechanical behavior and
 121 particle crushing of irregular granular material under high pressure using discrete element
 122 method. *Scientific Reports*, 13(1), 7843.
- 123 Dosta, M., André, D., Angelidakis, V., Caulk, R. A., Celigueta, M. A., Chareyre, B., Dietiker, J.-
 124 F., Girardot, J., Govender, N., Hubert, C., & others. (2024). Comparing open-source DEM
 125 frameworks for simulations of common bulk processes. *Computer Physics Communications*,
 126 296, 109066.
- 127 Govender, N., Wilke, D. N., & Kok, S. (2016). Blaze-DEMGPU: Modular high performance
 128 DEM framework for the GPU architecture. *SoftwareX*, 5, 62–66.
- 129 Harmon, J. M., Karapiperis, K., Li, L., Moreland, S., & Andrade, J. E. (2021). Modeling

- 130 connected granular media: Particle bonding within the level set discrete element method.
131 *Computer Methods in Applied Mechanics and Engineering*, 373, 113486.
- 132 Huang, T.-W., Lin, D.-L., Lin, C.-X., & Lin, Y. (2021). Taskflow: A lightweight parallel and
133 heterogeneous task graph computing system. *IEEE Transactions on Parallel and Distributed
134 Systems*, 33(6), 1303–1320. <https://doi.org/10.1109/TPDS.2021.3104255>
- 135 Jha, Prashant K., Desai, P. S., Bhattacharya, D., & Lipton, R. (2021). Peridynamics-based
136 discrete element method (PeriDEM) model of granular systems involving breakage of
137 arbitrarily shaped particles. *Journal of the Mechanics and Physics of Solids*, 151, 104376.
138 <https://doi.org/10.1016/j.jmps.2021.104376>
- 139 Jha, Prashant K., & Diehl, P. (2021). NLMech: Implementation of finite difference/meshfree
140 discretization of nonlocal fracture models. *Journal of Open Source Software*, 6(65), 3020.
141 <https://doi.org/10.21105/joss.03020>
- 142 Jha, Prashant K., Diehl, P., & Lipton, R. (2025). Nodal finite element approximation of
143 peridynamics. *Computer Methods in Applied Mechanics and Engineering*, 434, 117519.
- 144 Jha, Prashant K., & Lipton, R. (2018a). Numerical analysis of nonlocal fracture models in
145 holder space. *SIAM Journal on Numerical Analysis*, 56(2), 906–941. <https://doi.org/10.1137/17M1112236>
- 147 Jha, Prashant K., & Lipton, R. (2018b). Numerical convergence of nonlinear nonlocal
148 continuum models to local elastodynamics. *International Journal for Numerical Methods
149 in Engineering*, 114(13), 1389–1410. <https://doi.org/10.1002/nme.5791>
- 150 Jha, Prashant K., & Lipton, R. (2019). Numerical convergence of finite difference approx-
151 imations for state based peridynamic fracture models. *Computer Methods in Applied
152 Mechanics and Engineering*, 351, 184–225. <https://doi.org/10.1016/j.cma.2019.03.024>
- 153 Jha, Prashant K., & Lipton, R. P. (2020). Kinetic relations and local energy balance for
154 LEFM from a nonlocal peridynamic model. *International Journal of Fracture*. <https://doi.org/10.1007/s10704-020-00480-0>
- 156 Littlewood, D. J., Parks, M. L., Foster, J. T., Mitchell, J. A., & Diehl, P. (2024). The
157 peridigm meshfree peridynamics code. *Journal of Peridynamics and Nonlocal Modeling*,
158 6(1), 118–148.
- 159 Smilauer, V., Angelidakis, V., Catalano, E., Caulk, R., Chareyre, B., Chèvremont, W., Doro-
160 feenko, S., Duriez, J., Dyck, N., Elias, J., Er, B., Eulitz, A., Gladky, A., Guo, N., Jakob, C.,
161 Kneib, F., Kozicki, J., Marzougui, D., Maurin, R., ... Yuan, C. (2021). Yade documentation
162 (3rd edition). Zenodo. <https://doi.org/10.5281/zenodo.5705394>
- 163 Thompson, A. P., Aktulga, H. M., Berger, R., Bolintineanu, D. S., Brown, W. M., Crozier, P.
164 S., in 't Veld, P. J., Kohlmeyer, A., Moore, S. G., Nguyen, T. D., Shan, R., Stevens, M. J.,
165 Tranchida, J., Trott, C., & Plimpton, S. J. (2022). LAMMPS - a flexible simulation tool for
166 particle-based materials modeling at the atomic, meso, and continuum scales. *Computer
167 Physics Communications*, 271, 108171. <https://doi.org/https://doi.org/10.1016/j.cpc.2021.108171>
- 169 Zhang, R., Tagliafierro, B., Vanden Heuvel, C., Sabarwal, S., Bakke, L., Yue, Y., Wei, X.,
170 Serban, R., & Negruț, D. (2024). Chrono DEM-Engine: A discrete element method
171 dual-GPU simulator with customizable contact forces and element shape. *Computer
172 Physics Communications*, 300, 109196. <https://doi.org/https://doi.org/10.1016/j.cpc.2024.109196>